SAR INTERFEROMETRIC ANALYSIS OF GROUND DEFORMATION AT SANTORINI VOLCANO (GREECE)

Papageorgiou Elena [(1)], Foumelis Michael [(2)], Parcharidis Issaak [(2)]

[(1)] National and Kapodistrian University of Athens, Department of Geophysics and Geothermics, 15784 Zografou, Greece, Email: epapageo@geol.uoa.gr
[(2)] Harokopio University of Athens, Department of Geography,70, El. Venizelou Str., 17671 Athens, Greece, Emails: mfoumelis@hua.gr, parchar@hua.gr

ABSTRACT

The core of the present study builds on ground deformation monitoring by SAR Interferometry at Santorini Volcanic Complex (Greece). Dataset used for this case study, include the entire archive of ERS SAR and ENVISAT ASAR data for both ascending and descending orbits covering almost two decades of observations (1992-2010). Deformation signals of millimeter-level accuracy were retrieved from both SAR and ASAR datasets, by way of the Interferometric Stacking technique. The linear rate of differential phases and the corresponding errors were estimated by averaging the unwrapped differential interferograms. Subsequently, vertical deformation rates were calculated by the combination of LOS measurements in ascending and descending acquisition geometries. The observed ground deformation shows mainly subsidence in the central part of Santorini Caldera, at Nea Kammeni Island, equal to -5.1 ±0.7 mm/yr, and -6.3 ±1.2 mm/yr for the periods 1992-2000 and 2003-2010 respectively, while both signs of movements (uplift and subsidence) of lower scale magnitude were recognized elsewhere on the volcano. In fact, higher deformation rates for the period after 2003 (ranging between -4.6 mm/yr and 5.6 mm/yr), compared to the lower values of the period 1992-2000 (from -1.7 mm/yr to 2.7 mm/yr), indicate increase in the undergoing deformation of the volcanic complex. Finally, this work presents an attempt to obtain integrated interferometric results of ground deformation from both ERS and ENVISAT sensors in order to allow future investigations on the deformation sources of the volcanic complex, which could be further exploited in the volcanic hazard and risk assessment.

1. INTRODUCTION

Synthetic Aperture Radar (SAR) Interferometry has proven to be an important tool for mid- to long-term monitoring of active volcanoes [1], [2], [3] and [4], as it provides the two-dimensional of the three-dimensional deformation field. SAR Interferometry (InSAR) technique is a relatively newly developed technique, capable to measure ground deformation with subcentimeter precision and spatial resolution of tens-of-meters over large areas (100×100 km).

InSAR techniques such as Differential Interferometry (DInSAR) and Interferometric Stacking (IS) are prone to this direction. The standard DInSAR configuration analyses a single differential interferogram derived from a pair of SAR images. Apart from the simplest DInSAR configuration, the IS technique improves the quality of the DInSAR results since it makes use of large data-sets of SAR images.

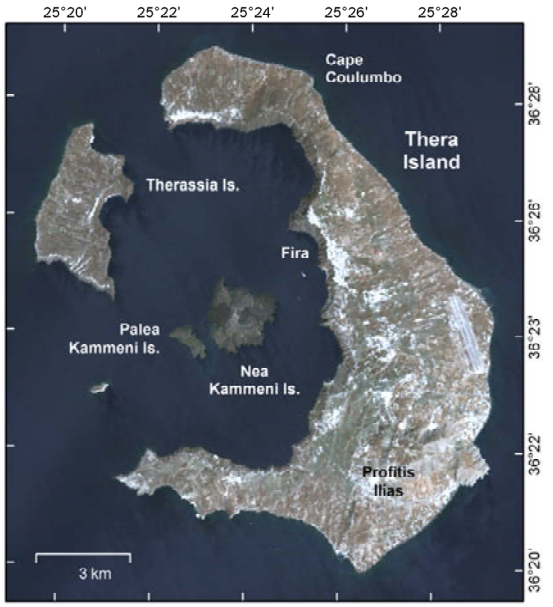

Figure 1. Santorini Volcanic Complex (SVC).

Our case study, the Santorini Volcanic Complex (SVC) (Fig. 1) is the most active volcanic center of the Hellenic Volcanic Arc at south Aegean Sea. It is a very complex stratovolcano and it is documented to have given numerous volcanic eruptions associated with caldera collapses, intense and strong seismic activities (6-7R), and tsunamis [5]. The eruption of Santorini in 1645 BC, one of the world's worst volcanic eruptions, destroyed completely entire civilizations on adjacent islands. During the last years there is little evidence that Santorini is in a permanent rest state. The SVC exhibits on-going seismic activity, and both fumaroles and hydrothermal springs are common features on the complex.

Proc. 'Fringe 2011 Workshop', Frascati, Italy,
19–23 September 2011 (ESA SP-697, January 2012)

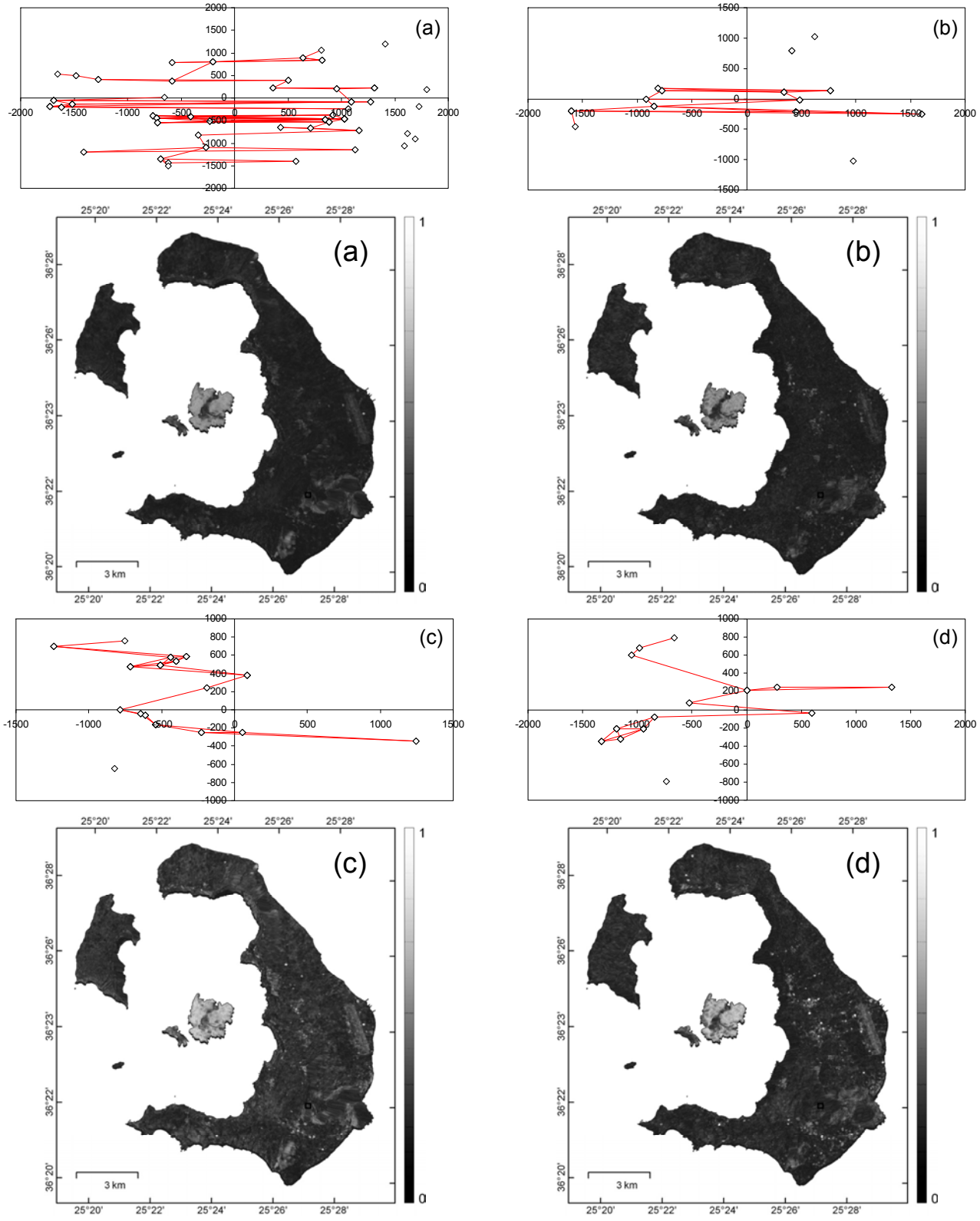

Figure 2. Temporal separation (x-axis, in days) versus perpendicular baseline (y-axis, in meters) plots, showing the available SAR data for the different datasets a) ERS descending (1992-2000), b) ERS ascending (1992-2000), c) ENVISAT descending (2003-2010) and d) ENVISAT ascending (2003-2010). The differential interferograms considered in the analysis based on baseline minimization criteria are indicated (red lines). The corresponding average coherence for each stack of interferograms is also shown.

Any kind of volcanic activity causes changes in the state of the volcano that is either uplift or subsidence. Hence, the study of the ground deformation in SVC, as it can be considered a precursory sign of magma intrusions, is crucial in the case of an impending eruptive activity.

The goal of this paper is to investigate the contemporary ground deformation field of the SVC including possible slope instabilities along the caldera walls that consists an important hazard and risk at the area [6], though settlements are situated along the edge of the caldera walls. In this attempt, IS technique was implemented to derive the ground deformation rates of the SVC, during the monitoring period 1992-2010. This enabled the identification of several domains with different displacement characteristics, which will be further discussed and interpreted herein.

2. GEODYNAMIC SETTING

Santorini lies in an area of complex extensional and subduction-related tectonics in a continental environment [7]. The current geodynamic state of SVC is controlled by two major volcanoes, the Nea Kammeni Volcano built up in the central caldera and the submarine Columbos Volcano, 7 km NE of Cape Columbos.

Volcanic activity is dated at least 1.6 Ma BP [8], and in the present day (last registered eruption in 1950) is characterized by superficial thermal manifestations (fumaroles and hot springs) in the internal part of the caldera as well as at the external side of the island. However, the presence of the high concentration of iron oxides inside the caldera, 3 km NE of Nea Kammeni, indicate a submarine hydrothermal vent [9]. It provoked intense seismic sequences and strong earthquakes have been registered. The current seismicity however, represents high seismic activity in the surrounding of Columbos Volcano area and fairly low seismic unrest at the rest of the complex [10]. What is particularly significant is the highest concentration of seismic hypocenters up to a depth of 15 km beneath the Columbos Volcano, a fact that is not revealed at Nea Kammeni Volcano. These recent seismological data indicate the existence of a magmatic champer below Columbos Volcano at depths of 6-9 km [10].

3. InSAR PROCESSING

3.1. SAR DATA

Data obtained from ERS -1 & -2 and ENVISAT satellites were used in this case processing covering the period from 1992 to 2010. ERS SAR acquisitions consists of 49 ERS-1 & -2 scenes in descending mode (track 150) and 16 in ascending mode (track 329) covering the period 1992-2002, as well as 17 and 14 ENVISAT ASAR scenes (ERS-like) in descending and ascending orbits of the same tracks respectively, for the period 2003-2010 (Fig. 2). The dates of the scenes and the diagrams presenting the interferometric pairs are shown in Fig. 2. GAMMA s/w packages were used for the processing [11]. As it is more a toolbox that supports different analysis approaches, adaptation to the processing requirements of the specific dataset was followed.

3.2. METHODOLOGY

Critical parameters considered primarily were to have an appropriate timeframe where the interferometric baselines are suitable in order to apply InSAR technique. Within the scope of this work, there are sufficient acquisitions in the archive to perform a more advanced interferometric technique such as IS that requires a large stack of interferograms promising for long timescale analysis over the area.

A considerable effort was given to accurately co-register the datasets, as this step affects significantly the robustness of subsequent processing. An oversampling of the original SLCs by a factor of 2 was considered appropriate, though precision measurement of the offset field is necessary. First attempt to estimate the range and azimuth registration offset field for pairs of SLC data, using the intensity cross correlation optimization technique, did not lead to satisfactory accuracies with estimated errors exceeding the pixel size. An alternative procedure based on fringe visibility, implementing coherence optimization algorithm was followed. Despite the advantages that the offsets are actually based on the interferometric phase coherence and no features are essentially required, poor results were achieved. This is primarily due to the significant loss of coherence after almost the first 2-3 years, for major parts of the SVC (except from Nea Kammeni).

Sufficient accuracies where achieved by applying a procedure, not only based on the correlation properties of two images, but also with the aid of an external DEM in range-Doppler SAR geometry [11]. By this means, offsets due to topography are taken into account. In some cases manual assistance of the co-registration steps was still compulsory. During co-registration, scenes of the same acquisition geometry, independently of the satellite sensor, where registered to a common master selected in the middle of each temporal dataset. Residuals calculation has shown an average sub-pixel level accuracy of about 1/8 and 1/5 of a pixel for range and azimuth, respectively. A transformation matrix between SAR and map coordinates in the co-registration step is also critical for geocoding the InSAR results to the selected map projection, without the need of the less accurate orbital data.

Initial estimates of the interferometric baselines were

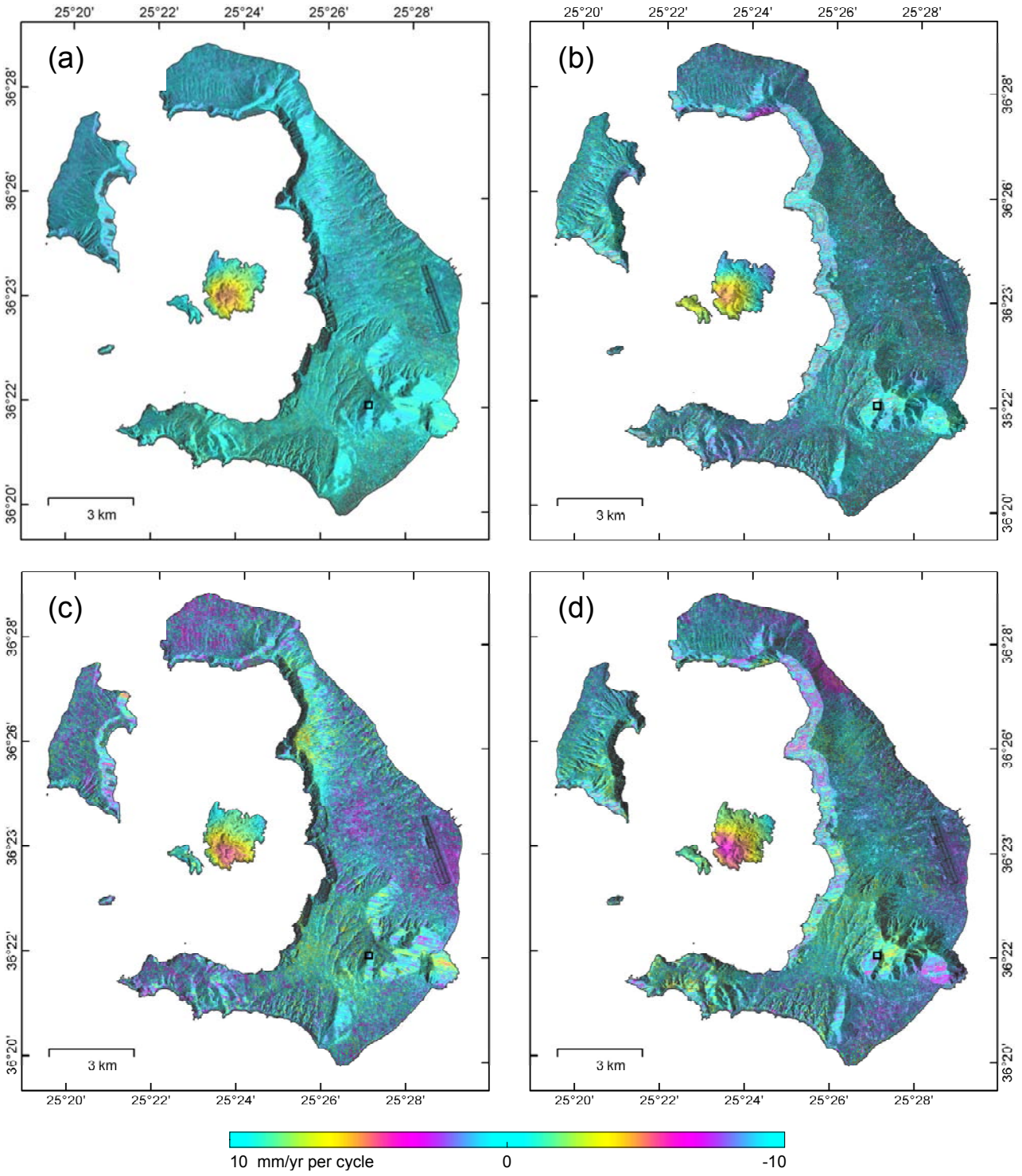

Figure 3. Ground deformation rates along the LOS direction deduced by interferometric stacking, for the considered time intervals and the different acquisition geometries as shown in Fig. 2. In background the corresponding average multi-looked SAR intensities. The selected reference point is shown in square.

available through DORIS and DELFT precise orbit state vectors. Due to the insufficient number of state vectors provided, additional state vectors with an interval of 5.0s were introduced by interpolation and orbit propagation. Data processing was limited to interferometric pairs that satisfy specific criteria with respect to perpendicular baseline (Bp). An upper limit for the Bp component of 100 m was considered, however, higher values (up to 150 m) had to be accepted in order to obtain sufficient number of

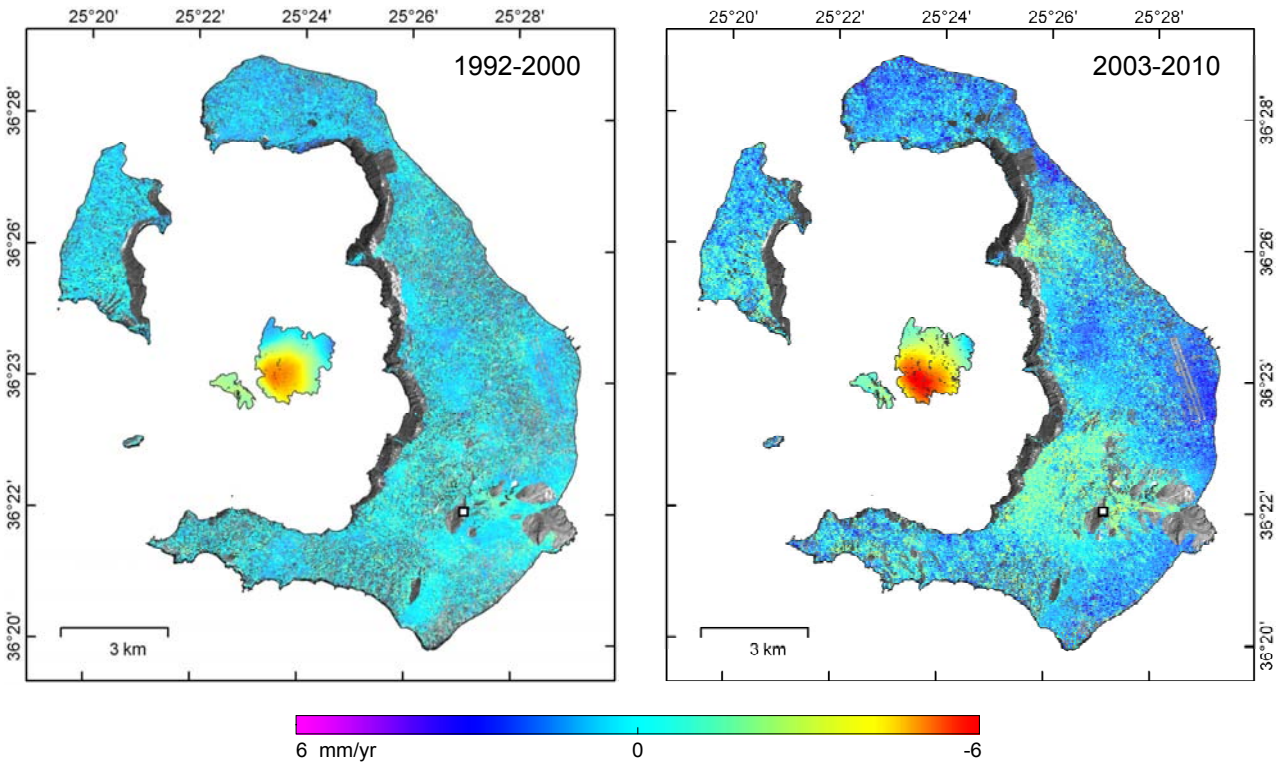

Figure 4. Vertical ground deformation derived from the combination of different SAR acquisition geometries, for the periods 1992-2000 and 2003-2010. The selected reference point is shown in square.

interferometric pairs for tracks with fewer scenes (Fig. 2). Additionally, to maintain a connected set of observations, selected interferograms with higher perpendicular baselines and short temporal separation were generated. Yet, few scenes with significant distance, in terms of spatial baseline, from the rest of the stack were not utilized (Fig. 2).

The main processing schema involves the generation of differential interferograms, filtering [12], spatial unwrapping using the Minimum Cost Flow algorithm [13], and refinement of the baseline information. Topography related phases were simulated and subtracted based on SRTM V3 DEM of approximate 90 m spatial resolution [14], which was oversampled to 20 m in order to fit with that of SAR data.

Several restrictions were encountered during processing. Visual inspection and exclusion of interferograms with spatial unwrapping errors was performed. These were mainly interferograms of large temporal baselines that exhibit considerable decorrelation phenomena. In addition, acquisitions of ERS-2, spanning from 2001 to 2002, were excluded due to the noise levels in the produced interferometric pairs, possibly related to Doppler variations. Similarly, two ERS scenes of 19920616 and 19991102 were also excluded due to recognized atmospheric phases.

Stacking is subsequently used to estimate the linear rate of differential phase, using a set of unwrapped differential interferograms. The individual interferogram phases when estimating the phase rate are weighted by the time interval. The underlying assumption is that atmospheric statistics are stationary from one observation to the next. Hence, the standard deviation of the phase rate derived from a single interferogram is proportional to 1/dt. Therefore, differential interferograms for each of the datasets were stacked by averaging, obtaining the estimation of the deformation rates and of the corresponding errors. Atmospheric phase contributions should be negligible or at least significantly minimized.

Since the phase measurements must be relative to a spatial reference point, in that case a GPS station from a local geodetic network [15], [16], was selected, serving future exploitation of both datasets. It is located at the south-eastern part of the island at Pygros Mt., where the Alpine basement outcrops. Typically the error of the estimated displacement rates will increase with increasing distance from the reference point, as the contribution of the phase errors due to atmosphere and baseline error increases. However, given the extent of the SVC (15 km × 17 km) such effects could be considered negligible. The ground deformation rates

obtained for the different periods and acquisition geometries are shown in Fig. 3.

Differential SAR interferometry permits to estimate the deformation component in SAR look direction. It is possible to calculate the vertical deformation rate vector based on the combination of ascending and descending orbits, and an additional assumption on the displacement direction. The constraint is that the motion vector points towards a central axis. This is an adequate assumption for concentric deformation pattern as may occur under certain circumstances such as subsidence and volcanic deformation. The results of such a combination for the time intervals examined are presented in Fig. 4. Although interpolation over layover and shadow areas for each stacking result was applied, it was decided not to include such areas affected by acquisition geometry, avoiding the introduction of errors in the final products. These localities correspond mainly to the mountainous regions at the sourth-eastern part of Thera, as well as the caldera steep slopes along the central part, facing toward the East or West.

3.3. RESULTS – INTERPRETATION

The products of the stacking method involve four deformation rate maps in LOS direction (Fig. 3). These maps which were produced by the stack of 60 and 17 differential interferograms for the period before 2000 (ERS descending & ascending, respectively), and 16 and 25 for the period after 2003 (ENVISAT descending & ascending, respectively) are presented in Fig. 3.

Generally, the optimal results as was expected due to the high coherence levels were observed at Nea Kammeni, at the center of the caldera, where systematic subsidence is indicative in all cases. In particular, concentric pattern of deformation denote prevalent subsidence in the southern part of Nea Kammeni. This subsidence amounts to -4.8 ±0.4 mm/yr for ERS descending case (Fig. 3a), -4.9 ±1.0 mm/yr for ERS ascending case (Fig. 3b), -5.7 ±1.1 mm/yr for ENVISAT descending case (Fig. 3c), and -6.7 ±0.9 mm/yr for ENVISAT ascending case (Fig. 3d). Moreover, substantial patterns of deformation were also observed in other parts of SVC. Among these a characteristic deformation pattern is observed in the ascending orbits of both ERS and ENVISAT sensors, located at the NW caldera walls, near Fira region (Fig. 3). While in the ERS deformation map the area seems to uplift, in the ENVISAT occasion the motion has been reversed. As far as it concerns descending orbits, a noticeable increase in the deformation rates is observed afterwards 2003. Therefore, the ERS results show smaller rates that range between 2.4 mm/yr and -4.8 mm/yr, than ENVISAT results that yield higher velocity rates, that is from 8 mm/yr up to -6.6 mm/yr. The latter suggests by some means, rather stable conditions before 2000, where the average velocity rate all around the SVC ranges from 2 mm/yr to -2 mm/yr. On the other hand, the larger values of deformation after 2003 indicate two zones of immense subsidence with rates of -6 mm/yr at the central and south parts of SVC, as well as considerable uplift of 7 mm/yr at the central-east part of SVC. These distinct features are also recognizable prior to 2000, but not to this sizable extent.

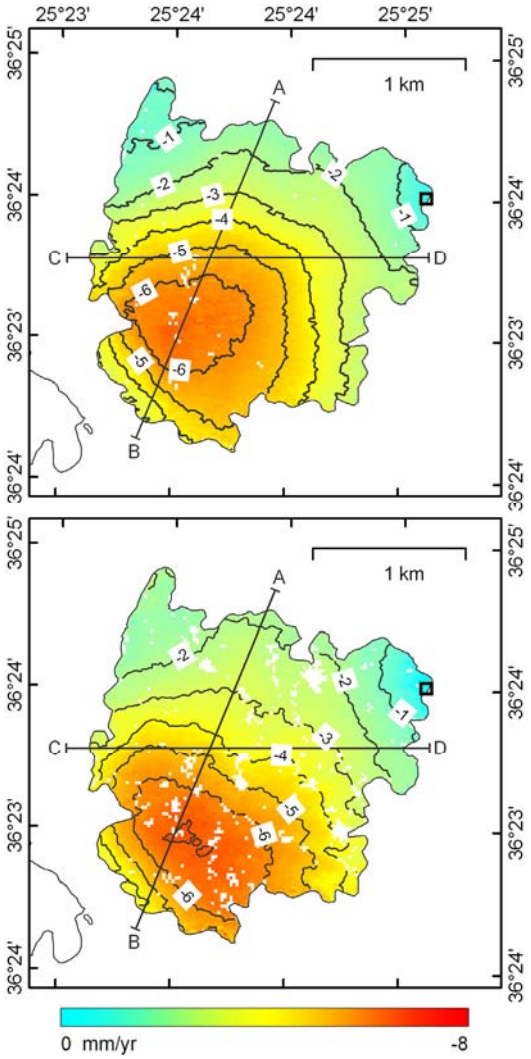

Figure 5. Ground deformation rates at Nea Kammeni, where the maximum subsidence is displayed for the periods 1992-2000 (up) and 2003-2010 (down). For presentation purposes a local reference point (square) was selected.

As far as it concerns the vertical deformation rates common subsidence is shown in Nea Kammeni for both periods, which in specific, earlier to 2000 is equal to -5.1 ±0.7 mm/yr, while after 2003 increases to -6.3 ±1.2 mm/yr (Fig. 4). Apparently, when referring to a local reference point located at the north-eastern part, where uplift is observed, a relatively increasing subsidence is occurring from the north to the south resulting to a

relative differential deformation of 6.9 mm/yr and 7.2 mm/yr (Fig. 5, 6). The rest of SVC shows almost similar deformation pattern which becomes more intense later to 2003. The velocity rates vary from -1.7 mm/yr to 2.7 mm/yr before 2000 and -4.6 mm/yr to 5.6 mm/yr after 2003. Thus, two significant zones of subsidence are observed in the central and south part of SVC, whereas for the most part uplift is evident, with particularly higher rates in central-east and north SVC. It should be noticed that the average errors for the interval 1992-2000 were at the order of ±0.6 mm/yr. The higher average uncertainties (±1.2 mm/yr) for 2003-2010 are attributed to the lower number of stacked pairs.

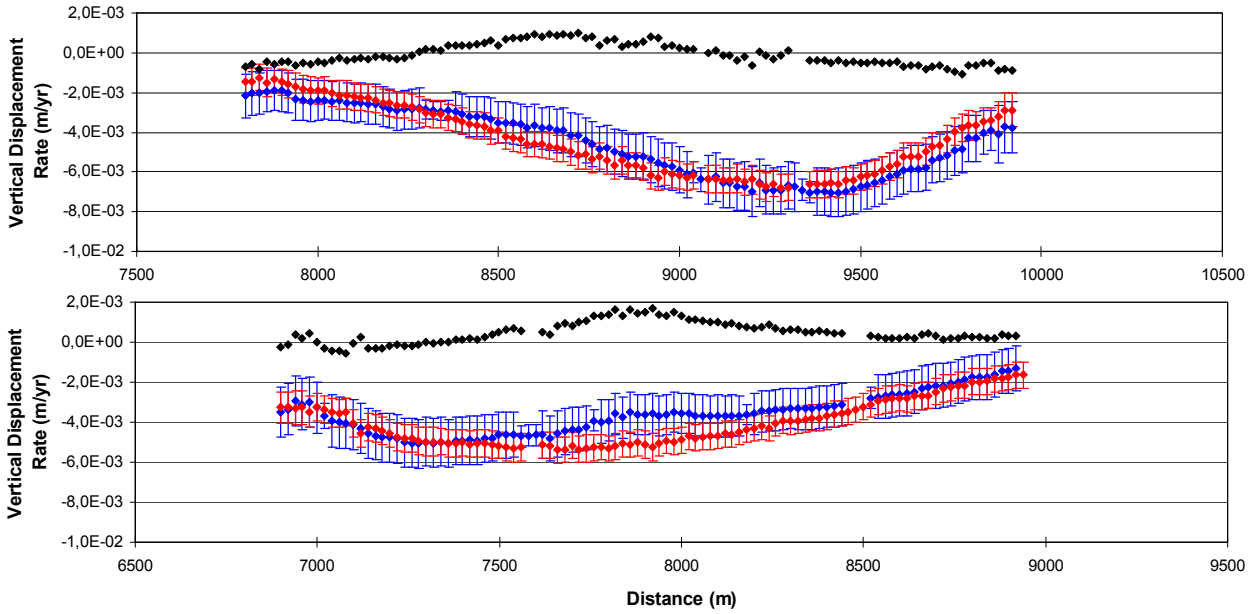

Figure 6. Spatial profiles A-B and C-D of the vertical deformation rates at Nea Kammeni as shown in Fig. 5, for the periods 1992-2000 (red) and 2003-2010 (blue), as well as their differences (black). Bars represent the 1-sigma standard deviation of the estimated vertical rates.

A noteworthy argument is the loss of information at caldera walls. Ascending data cover some portions of the caldera walls, while descending data cover the remaining parts and no joint areas are finally conformed. Hence, no common information is finally achieved and to this end the areas with layover and shadow are not finally chosen to be entered in the calculation of the vertical motion.

4. DISCUSSION

In this paper IS technique has been applied for the first time in SVC, in order to monitor the ground deformation. The key benefit was to exploit large sets of SAR images acquired over the same area, that minimize error contributing factors, such as the atmospheric delays. Furthermore, the large number of ERS and ENVISAT archive acquisitions allows the optimization of the data selection with respect to the interferometric baselines and the temporal separation.

In advance, the large datasets of SAR and ASAR images of different viewing geometries enable the calculation of the accurate vertical velocity of SVC throughout the entire period of 18 years, i.e. from 1992 to 2010. This significant topic is receiving particular attention, as the vertical information can be integrated to GPS monitoring networks operating at the region [15]. Still when referring to the quality of the GPS results, some limitations arise in the vertical component, and more precise validation is required with the contribution of the relatively more accurate SAR interferometric observations. This will permit a more accurate description of the three dimensional (3D) deformation field of the region.

The results show common deformation patterns for both periods, before 2000 and after 2003. However, the deformation rates indicate higher values for the period after 2003. Briefly summarizing, characteristic subsidence phenomena are observed in Nea Kammeni, at the center of the caldera, implying maximum relative deformation rates at the southernmost part of the island. Additionally, two pronounced regions of subsidence are recognized in Thera with rather notable rates. Peculiar uplift effects of considerable deformation rates were also identified in north and eastern Thera.

The main limitations of the interferometric technique when estimating the accurate vertical deformation, by the combination of both the ascending and descending mode, appeared to be the exclusion of areas of rugged topography, affected by layover and shadow. In our case, Santorini caldera walls with immensely steep slopes of approximately 300 m were excluded and no information is provided, whereas it would be useful in landslide monitoring. This should be considered as a limited factor for vertical motion detection when investigating the slope instabilities at these areas through spaceborne SAR interferometry. Nevertheless, stacking results in LOS direction are still promising towards this direction.

The region exhibits considerable decorrelation even for short temporal interferometric pairs. This fact underlines the effects of the seasonal variations of its land cover characteristics. Therefore, certain complications arise when SAR interferometry is applied for deformation monitoring. However, considering the plethora of the existing data, a quite robust solution was finally achieved.

State-of-the-art interferometric technique of Persistent Scatterers Interferometry (PSI), yet beyond the scope of this paper, is considered to be performed at a future date in order to investigate temporal variations of the deformation field.

5. ACKNOWLEDGEMNTS

The present study was carried out within the frame of ESA's Announcement of Opportunity (A.O.) project for Greece.

6. REFERENCES

1. Massonnet, D. & Feigl, K.L. (1998). Radar interferometry and its application to changes in the Earth's surface. *Rev. Geophys*. **36**, 441-500.
2. Bürgmann, R., Rosen, P.A. & Fielding, E.J. (2000). Synthetic Aperture Radar Interferometry to measure Earth's Surface Topography and its Deformation. *Ann. Rev. Eath Planet. Sci*. **28**, 169–209.
3. Hanssen, R. (2001). *Radar Interferometry: Data Interpretation and Error Analysis*. Kluwer Academic Press, Dordrecht. The Netherlands, 298pp.
4. Lagios, E., Parcharidis, Is., Foumelis, M. & Sakkas, V. (2005). Ground deformation monitoring of the Santorini volcano using satellite radar interferometry. Proceedings of 2nd International Conference on Recent Advances in Space Technologies (RAST 2005), 667-672.
5. Antonopoulos, J. (1992). The great Minoan eruption of Thera volcano and the ensuing tsunami in the Greek archipelago. *Natural Hazards* **5**, 153-168.
6. Lekkas, E. (2009). Landslide hazard and risk in geologically active areas. The case of the caldera of the Santorini (Thera) volcano island complex (Greece). Proceedings of the 7th Asian Regional Conference of IAEG, Chengdu, China, 417-423.
7. Jackson, J.A. (1994). Active tectonics of the Aegean region. *Annual Reviews of Earth and Planetary Sciences* **22**, 239-271.
8. Ferrara, G., Fytikas, M., Guiliano, O. & Marinelli, G. (1980). Age of the formation of the Aegean active volcanic arc. In: Doumas C. (ed). Thera and the Aegean World II, 37-41.
9. Sigurdsson, H., Carey, S., Alexandri, M., Vougioukalakis, G., Croff, K., Roman, C., Sakellariou, D., Anagnostou, C., Rousakis, G., Ioakim, C., *Gogou, A., Ballas, D., Misaridis, T. & Nomikou P.* (2006). New marine geological investigations of the Santorini volcanic field. *Eos Transactions, American Geophysical Union* **87**, 337–342.
10. Dimitriadis, I., Karagianni, E., Panagiotopoulos, D., Papazachos, C., Hatzidimitriou, P., Bohnhoff, M., Rische, M. & Meier T. (2009). Seismicity and active tectonics at Coloumbo Reef (Aegean Sea, Greece): Monitoring an active volcano at Santorini Volcanic Center using a temporary seismic network. *Tectonophysics* **465**, 136-149.
11. Wegmüller, U, Werner, C. & Strozzi T. (1998). SAR interferometric and SAR differential interferometric processing chain. Proceedings of IGARSS, v.2, 1106-1008.
12. Goldstein, R. & Werner, C. (1998). Radar interferogram filtering for geophysical applications. *Geophysical Research Letters* **25**(21), 4035-4038.
13. Costantini, M. (1998). A novel phase unwrapping method based on network programming. *IEEE Transactions on Geoscience and Remote Sensing* **36**(3), 813-821.
14. Jarvis, A., Reuter, H.I., Nelson, A. & Guevara, E. (2006). Hole-filled seamless SRTM data V3, International Centre for Tropical Agriculture (CIAT), available from http://srtm.csi.cgiar.org.
15. Papageorgiou, E. (2011). Surface Deformation Study for the Volcanic Hazard Assessment using Geophysical and Space Techniques: The Case of the Hellenic Volcanic Arc. Doctorate Thesis, University of Athens (in Greek).
16. Papageorgiou, E., Tzanis, A., Sotiropoulos, P. & Lagios, E. (2010). DGPS and magnetotelluric constraints on the contemporary tectonics of Thera Island, Greece. Bull. Geol. Soc. Greece, XLIII, 1, 344-356.